LIGHT TRAPPING IN SUNPOWER'S A-300 SOLAR CELLS

Keith R. McIntosh,[1] Nicholas C. Shaw[2] and Jeffrey E. Cotter[2]
[1] SunPower Corporation, 430 Indio Way, Sunnyvale, CA 94085, U.S.A.; ph.: +1 408 991 0900
[2] Centre for Photovoltaic Engineering, University of NSW, 2056, AUSTRALIA; ph.: +61 2 9385 4062

ABSTRACT: Light trapping in SunPower's A-300 solar cells was experimentally investigated by measuring the escape reflectance and the quantum efficiency. It is concluded that the cells have a rear-internal reflection of 75–80% and a pathlength enhancement of Z ~ 6, indicating relatively good light trapping. Several means to increase Z are explored—white paint, rear texture, and tilted front texture—but it is found that the subsequent increase in cell efficiency does not warrant the increase in process complexity. The primary reason for this is that, with random pyramids at the front surface and a planar rear surface, few photons intersect the rear surface within the escape angle an Si–SiO_2 interface; thus, a thick SiO_2 on the rear is sufficient to provide high internal reflection.
Keywords: Light trapping, Optical losses, High efficiency.

1 INTRODUCTION

SunPower is equipping its first factory to produce A-300 solar cells. The A-300 is a rear-contact solar cell with an efficiency greater than 20% and a grid-free front surface. Its structure, virtues, superiority and fabrication have been presented elsewhere [1]. Sales of the first cells are forecasted for the end of 2004.

This paper concerns the light-trapping of the A-300. We first calculate that the cell traps 93% of the available photons from the AM1.5g spectrum, which amounts to a generation current of 41.2 mA/cm^2. We then discuss how the light trapping might be increased by adding a reflector to the rear surface or by instituting changes to the texturing. It is concluded that while small improvements might be gained, it would not warrant the increased processing complexity. Instead, the best method to improve the light trapping is to raise the rear-internal reflection.

2 THE BENEFIT OF LIGHT TRAPPING

Light trapping makes the "optical thickness" of a solar cell greater than its actual thickness. This is achieved by (1) coercing light rays to pass obliquely through the cell; and (2) instituting a non-zero internal reflectance at the front and rear surfaces to prevent rays from escaping.

By making the optical thickness greater than the actual thickness, one forces the light rays to spend more time in the solar cell, which leads to a greater absorption of long-wavelength photons, and hence, a larger generation current J_G.

Figure 1 shows how J_G depends on the optical thickness of SunPower's A-300 solar cell for two cases: (i) unencapsulated, and (ii) encapsulated.

J_G was found by determining the light transmitted into the cell with an in-house optical model that utilises the matrix method outlined by Macleod [2], and by assuming the absorption coefficients for band-to-band absorption and free-carrier absorption as given by Reference [3] for silicon. The optical model assumes normally incident light, 100 mW/cm^2, AM1.5g spectrum [4], perfect pyramidic texture (54.75°) on the front surface, a TM:TE polarization fraction of 1:1, non-dispersive media, specula reflection, 300 Å of an SiO_2 passivation layer, and 450 Å of SiN. The transmission of the encapsulation was measured by SunPower for one layer of glass plus 0.2 mm of EVA; the values of $n(\lambda)$ and $k(\lambda)$ for SiO_2 were taken from Palik [5] and those of SiN were measured by spectroscopic ellipsometry from a PECVD SiN film deposited by Roth and Rau.

Figure 1 illustrates the large improvement in J_G that can be gained by increasing the optical thickness. For instance, if the cell were 250 µm thick with no light trapping, an unencapsulated cell would forgo almost 6 mA/cm^2 (13%) of the available generation current. If the same cell incorporated light trapping such that the optical thickness was 1500 µm (i.e., $Z = 6$), the loss in generation current would be halved to 3 mA/cm^2.

Light trapping is typically quantified by the pathlength enhancement factor Z, where Z is defined to be the optical thickness W_O divided by the cell thickness W:

$$Z = W_O / W .$$

The purpose of this work is to determine Z for SunPower's A-300 solar cell, and to explore economically viable ways to increase Z.

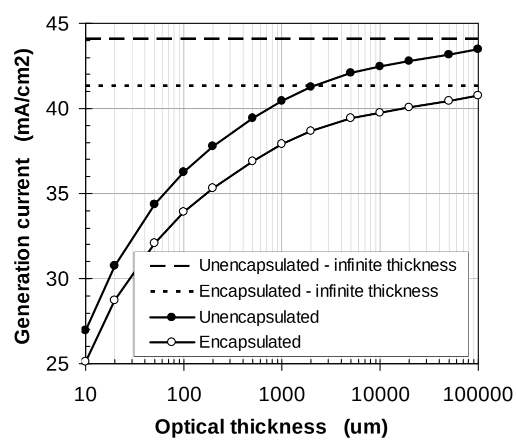

Figure 1: Generation current vs optical thickness for SunPower's A-300 solar cell under one-sun illumination; other assumptions are listed in the text.

3 LIGHT TRAPPING IN THE A-300

Figure 2 depicts the relevant features of the solar cells investigated in this study. The front surface is textured with random pyramids (54.75°) and coated with a passivating SiO_2 film and an anti-reflective film; the texture refracts the incident light so that it travels obliquely to the plane of the cell, thereby increasing the optical pathlength.

The rear surface is planar and coated with SiO_2 except where the metal makes contact to silicon. The metal constitutes the positive and negative electrodes, and it forms a pattern of interdigitated fingers over the most of the cell.

As a consequence of the metal pattern, there are three interfaces at the rear surface: (i) Si–metal at the contacts, (ii) Si–SiO_2–metal in the regions away from the contacts but still under the metal grid, and (iii) Si–SiO_2 in the regions between fingers. The proportion of the rear constituted by each interface is (i) 2.5%, (ii) 79% and (iii) 18.5%, for the cells of this study.

Ideally, we would like to derive an explicit equation to describe the optical thickness of the structure. But this approach is confounded by the pyramids at the front surface, which, as well as transmitting some fraction of a ray into the cell, reflects the remainder of the ray onto other pyramids. Thus, the front texture leads to the multiplication of rays, making the derivation of an explicit expression impossible. (The multiplication of rays occurs for both external and internal rays.)

We therefore resort to experimentation and computer ray tracing to ascertain the optical thickness of our cell. Before presenting the results, we describe some attributes of the structure.

Figure 2 shows the path of the most common ray, Ray A. Ray A is transmitted into the silicon and refracted by the pyramids to an angle of 41.4° to the normal of the rear surface (as calculated by Snell's law with n_{Si} = 3.54). This angle is larger than the critical angle (24.4°) of a Si–SiO_2 interface, so the ray is internally reflected. The ray then intersects the front surface at an opposing pyramid facet and is transmitted out of the cell. This ray has a pathlength enhancement of Z ~ 3.

Almost all other rays have additional interactions that lead to a greater pathlength enhancement: Some rays enter the cell after reflecting from one pyramid facet onto another, leading to a more oblique path through the cell; and some rays internally reflect from the front surface to traverse the width of the cell again. Thus, we expect the average pathlength enhancement to be greater than 3, and as described later, it is found to be Z ~ 6.

Light rays are lost from a cell when they are absorbed at an interface, or when they are transmitted out of the cell. At the front surface of this structure, there is no absorption at long wavelengths because the absorption coefficient of SiO_2 and the ARC is negligible; and there is little transmission because the pyramidic structure and the small critical angle make it difficult for rays to escape. (The exception is the first-pass rays, of which many intersect an opposing facet as shown by Ray A.)

At the rear surface, the absorption is low due to the high reflectivity of the Si–metal (~85%) and Si–SiO_2–metal interfaces (85–100% depending on the angle of incidence and thickness of SiO_2); and few rays are transmitted out of the cell. Rays can only escape if they intersect the rear surface between the interdigitated fingers (i.e., in the Si–SiO_2 regions) at an angle less than the critical angle, depicted as Ray B in Figure 2.

By modeling the cell with a freeware ray tracing program, RaySim [6], we found that the fraction of rays that escaped through SiO_2 was less than ~1% This small fraction is consistent with the experiment that follows.

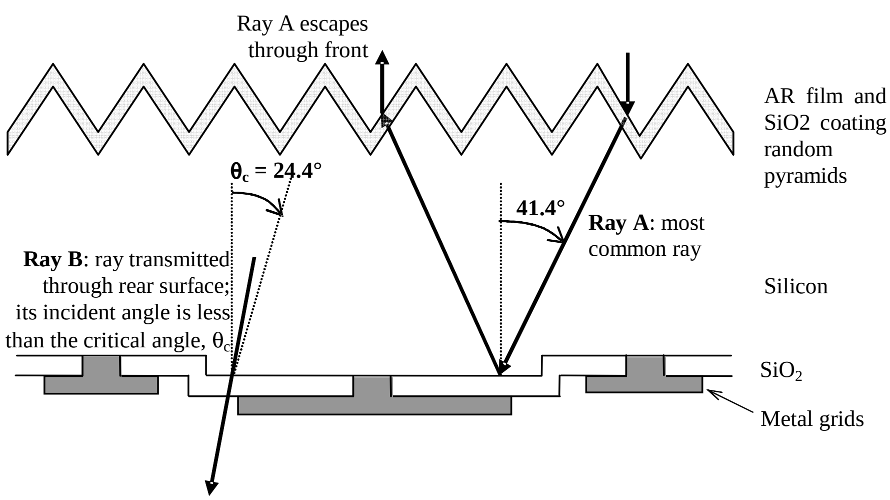

Figure 2: Schematic diagram of A-300 solar cell (not to scale).

4 EXPERIMENT

To assess the light trapping of the A-300, we measured the escape reflectance of four cells at long wavelengths ($1200 > \lambda > 1400$ nm). At these wavelengths, the band-to-band absorption of photons in silicon is negligible and therefore, once light enters the solar cell, it is only lost by being transmitted out of the front or rear of the cell, by being absorbed by the metal, or by free-carrier absorption in the silicon. (Absorption in the ARC and SiO_2 is negligible at these wavelengths.)

The escape reflectance was determined by measuring the total reflectance and removing the contribution of the external front reflection with the equation,

$$R_{escape} = (R_{measured} - R_{external}) / (1 - R_{external}).$$

In this way, only the light that enters the cell contributes to the escape reflectance. The external front surface reflection was determined by extrapolating the measured reflectance at 700–900 nm to longer wavelengths.

Figure 3 plots R_{escape} as a function of wavelength for two A-300 solar cells (solid symbols). For clarity, R_{escape} of the remaining two cells is not shown, but in both cases, it follows the same trend with similar values. At 1200 nm, the measured escape reflectance of all four cells was within the range, R_{escape} = 47–51%.

Figure 3 shows that R_{escape} decreases with increasing wavelength. One possible reason for this trend is that the photons of longer wavelengths interact more with the metal in the Si–SiO_2–metal stack, which decreases the rear reflection; this suggests that the rear SiO_2 is thinner than optimal. A second possibility is that free-carrier absorption is not negligible; using coefficients found in Ref [3], we calculated that at these wavelengths, FC absorption would be <1% in the bulk but could be higher in the diffusions. Either possibility infers that R_{escape} at 1000–1200 nm would be a little higher than at 1200 nm.

Figure 3 also plots R_{escape} after white paint was coated onto the rear surface of the cells. White paint, sometimes referred to as a pigmented diffuse reflector, has a high reflectance and reflects light with a small escape cone, irrespective of the angle of incidence [7]. The paint used in our study was measured to have a reflection of ~90% and an escape cone of ~15° at long wavelengths [8]. It is optically superior to encapsulated white tedlar, which has a ~70% randomised reflectance [8].

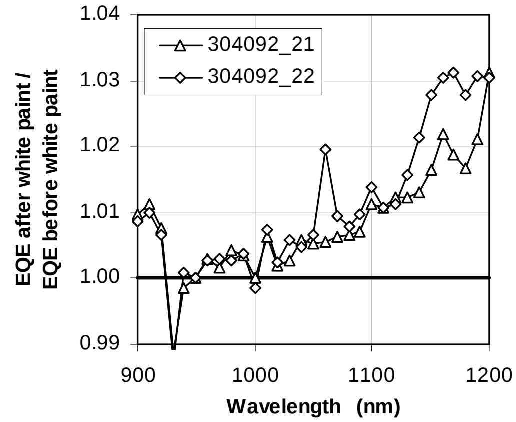

Figure 4: Change in *EQE* after coating the rear of the cells with white paint.

Thus, with white paint on the rear, 90% of the rays that would have escaped between the interdigitated fingers (Ray B in Figure 2), are reflected back into the cell at an angle that subsequently reflects at the front surface. The inclusion of the white paint should therefore increase the optical thickness of the cell.

The increase in optical pathlength can be seen in Figure 3, manifested as an increase in R_{escape} at long wavelengths; R_{escape} rose by 0.8–1.8% absolute at 1200 nm for all four samples.

It can also be seen in Figure 4, which plots the change in *EQE* of a small region of the same cells. Below 1100 nm, the change in *EQE* was ±1%, for which the rear reflectance is negligible; this was considered to be the error of the experiment. Above 1100 nm, there was a significant increase in *EQE*, which is consistent with an optically thicker cell. Multiplying $EQE(\lambda)$ by the AM1.5g spectrum indicates that the white paint would increase cell efficiency by $0.3 \pm 0.2\%$ absolute.

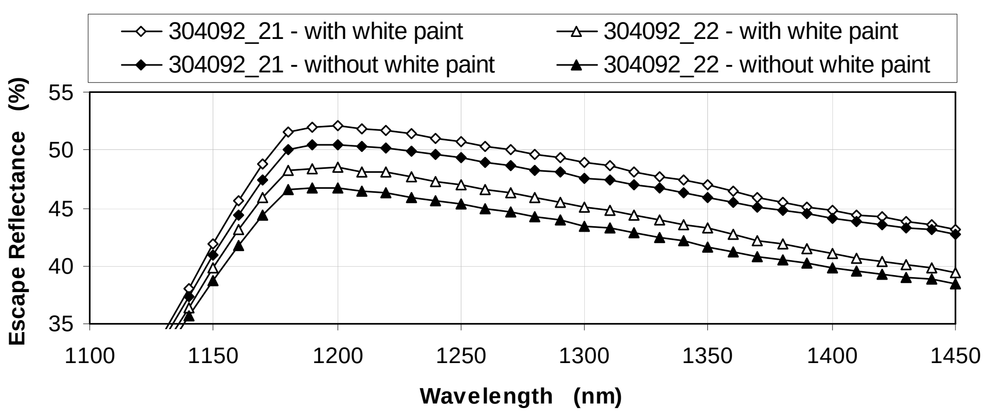

Figure 3: Experimental escape reflectance of two A-300 solar cells, measured before (solid symbols) and after (open symbols) the application of white paint on the rear surface.

Table 1: Escape reflectance R_{escape}, rear internal reflectance R_{rear}, pathlength enhancement Z, generation current J_G (one-sun) for samples with and without white paint, change in generation current ΔJ_G and absolute efficiency Δeff.

Sample	R_{escape} (%)		R_{rear} (%)		Z		J_G (mA/cm²)		ΔJ_G (mA/cm²)	Δeff (%)
	w/out	with	w/out	with	w/out	with	w/out	with		
304092-02	46.7	48.3	75.3	77.2	5.72	6.07	41.24	41.32	0.08	0.041
304092-06	46.1	46.9	74.6	75.5	5.60	5.78	41.22	41.25	0.03	0.015
304092-21	50.5	52.1	79.6	81.2	6.58	6.98	41.41	41.48	0.07	0.035
304092-22	46.7	48.5	75.3	77.4	5.72	6.11	41.24	41.32	0.08	0.041

5 CALCULATIONS

Table 1 summarises the results. As well as the escape reflectance R_{escape}, it lists five other calculated parameters: the rear internal reflection R_{rear}, the pathlength enhancement Z, the generation current J_G, the change in J_G, and the change in absolute efficiency Δeff.

To calculate R_{rear}, we first assumed that the front internal reflection R_{front} was 43% for the first bounce, 100% for the second, and 94% for subsequent bounces; these values approximate a modeled curve shown in Figure 6.8 of Reference [3] for the case of random pyramids and a specular rear surface. We then imposed a constant value of R_{rear} for all bounces and calculated the total fraction of rays that escaped from the front surface R_{escape}. Lastly, we adjusted R_{rear} until the calculated R_{escape} equaled the experimental R_{escape}. (We assumed no FC absorption.)

R_{rear} is therefore an average rear internal reflection for the whole rear surface and for all bounces. Although it is relatively high (75–80%), it is lower than the expected value at 1200 nm for the Si–metal (~85%) and Si–SiO_2–metal (85%–100%, depending on the angle of incidence and thickness of SiO_2). This cannot be entirely explained by transmission through the Si–SiO_2 regions because the inclusion of white paint increased R_{rear} to just 76–81%. A second effect that could have reduced R_{rear} below the expected value is alloying within the metals of the electrodes or between the metal and the silicon.

In our calculations, Z is a weighted average pathlength of the rays. It assumes that the distance of each pass is sin(41°) times the width of the cell, since 41° is the angle of the first and second passes. We conclude that Z ~ 6 for the A-300 and that it increases by just 0.2–0.4 with white paint on the rear surface.

J_G was determined from Figure 1 for the experimental cell thickness of W = 250 µm.

Finally, Δeff was determined by assuming that eff is proportional to J_G, which is reasonable for the A-300 because of its very long bulk lifetime (>2 ms). The calculated Δeff of Table 1 is consistent with the value determined from the *EQE* measurements in Section 4.

By following the same procedure, we also determined how alternative texturing might affect the efficiency for a range of R_{rear}. (Again, we set R_{front} to emulate modeled results in Ref. [3]). Table 2 lists the results. It shows that a small gain in efficiency is attainable by including pyramids on the rear, or tilted pyramids on the front; or by raising R_{rear} to the expected level for the metal.

Table 2: Z, J_G and eff calculated for a 250 µm thick A-300 solar cell for a range of R_{rear} and texture patterns.

R_{rear} (%)	Z	J_G (mA/cm²)	eff (%)	
Front: *random pyramids,* ***Rear:*** *planar*				
75	5.7	41.2	21.0	(baseline)
80	6.7	41.4	21.1	
85	8.1	41.7	21.3	
90	10.5	41.9	21.4	
Front: *random pyramids,* ***Rear:*** *random pyramids*				
75	7.1	41.5	21.2	
80	8.4	41.7	21.3	
85	10.0	41.9	21.4	
90	12.7	42.1	21.5	
Front: *24° tilted random pyramids,* ***Rear:*** *planar*				
75	7.8	41.8	21.3	
80	9.1	41.8	21.3	
85	10.9	41.9	21.4	
90	13.5	42.1	21.5	

6 CONCLUSION

The pathlength enhancement of SunPower's A-300 solar cell was determined to be Z ~ 6. For a 250 µm thick cell, this results in a generation current of J_G = 41.2 mA/cm² (93% of available photons) under one-sun illumination. The best way to improve these values is to increase the rear internal reflectance, possibly by thickening the rear SiO_2 or by limiting alloying of the metal electrodes. Z and J_G can be slightly improved by coating the rear surface with white paint or by altering the texturing patterns, but the economic advantage of raising the efficiency is probably outweighed by the cost of the added processing complexity. We also found that with random pyramids on the front surface and a specular planar rear surface, few rays intersect the rear surface within the critical angle, and therefore, few rays escape through the Si–SiO_2 regions; there is therefore little optical advantage to increasing the rear metal coverage.

7 REFERENCES

[1] W.P. Mulligan *et al.*, *Proc.19th EC PVSEC*, 2004; K.R. McIntosh *et al.*, *Proc. 3rd WCPEC*, 2003; M.J. Cudzinovic *et al.*, *Proc. 29th IEEE PVSC*, p. 70, 2002; and references therein.

[2] H.A. Macleod, *Thin Film Optical Filters*, 2nd ed., Adam Hilger Ltd., Ch. 2, 1986.

[3] M.A. Green, *Silicon Solar Cells*, UNSW, 1995.

[4] R. Hulstrom *et al.*, *Solar Cells* **15** (4), pp. 365, 1985.

[5] Palik, *Handbk of Optical Constants of Solids*, p 759.

[6] RaySim: www.pv.unsw.edu.au/jcotter/main.htm.

[7] J.E. Cotter, *Prog in PV* **7**, pp. 261–274, 1999.

[8] N. Shaw, *PhD Thesis*, UNSW, 2004.